

SUPPLEMENTARY MATERIAL for:
Ferrocenes with Simple Chiral Substituents: an
In-Depth Theoretical and Experimental VCD and
ECD Study

Angela Patti, Sonia Pedotti, Giuseppe Mazzeo, Giovanna Longhi, Sergio Abbate,
Lorenzo Paoloni, Julien Bloino, Sergio Rampino, Vincenzo Barone

Contents

1 S-1-acetoxyethylferrocene

- 1.1 Structure of each conformer
- 1.2 Assignment of normal modes of the most abundant conformer (T=298K)
- 1.3 Anharmonic calculations: frozen LAMs and added Fermi resonances
- 1.4 Calculated IR and VCD spectra of each conformer
- 1.5 Experimental ¹H NMR spectrum and assignment
- 1.6 coefficient of optical rotation: experimental values

2 S-1-methoxyethylferrocene

- 2.1 Structure of each conformer
- 2.2 Assignment of normal modes of the most abundant conformer (T=298K)
- 2.3 Anharmonic calculations: frozen LAMs and added Fermi resonances
- 2.4 Calculated IR and VCD spectra of each conformer
- 2.5 Experimental and computational spectra in the 1500-1900 cm⁻¹
region
- 2.6 Experimental ¹H NMR spectrum and assignment
- 2.7 coefficient of optical rotation: experimental value

3 S-1-hydroxyethylferrocene

- 3.1 Structure of each conformer
- 3.2 Assignment of normal modes of the most abundant conformer (T=298K)
- 3.3 Anharmonic calculations: frozen LAMs and added Fermi resonances
- 3.4 Calculated IR and VCD spectra of each conformer
- 3.5 Frequencies, IR intensities and rotational strength in the OH stretch-
ings region for each conformer

3.6	Experimental and computational spectra in the 1500-1900 cm^{-1} region
3.7	Calculated ECD and absorption spectra of each conformer (280-650 nm region)
3.8	Experimental ^1H NMR spectrum and assignment
3.9	coefficient of optical rotation: experimental value
3.10	Bond analysis on conformers I, II and III
3.10.1	Brief outline of the method
3.10.2	Computational details
3.10.3	Results
4	(S,S)-1,1'-bis(1-hydroxyethyl)ferrocene
4.1	Monomers
4.1.1	Structure of each conformer
4.2	Dimer
4.2.1	Structure
4.3	Experimental ^1H NMR spectrum and assignment
4.4	coefficient of optical rotation: experimental value
4.5	DOSY spectrum

1 S-1-acetoxyethylferrocene

1.1 Structure of each conformer

In this section the structure of each conformer from different perspectives is reported; each geometry is optimized at the B3PW91/Def2TZVP level of theory.

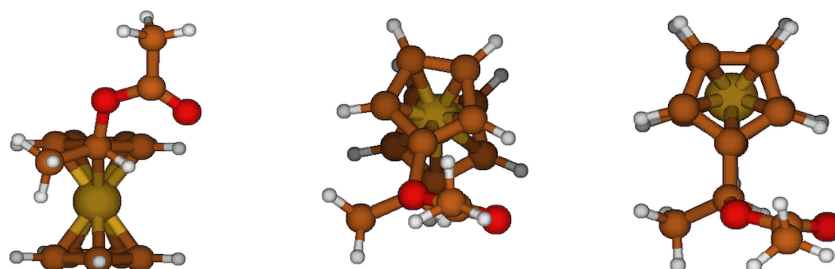


Figure SI 1: conformer I

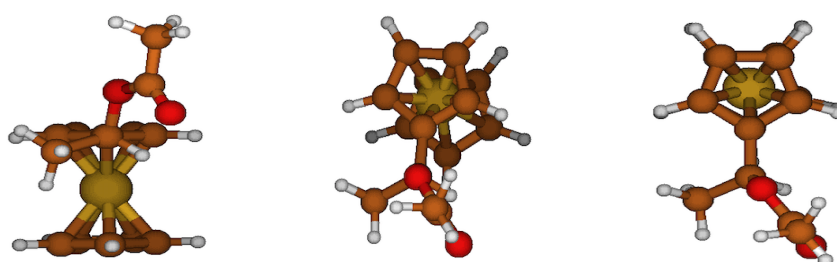


Figure SI 2: conformer II

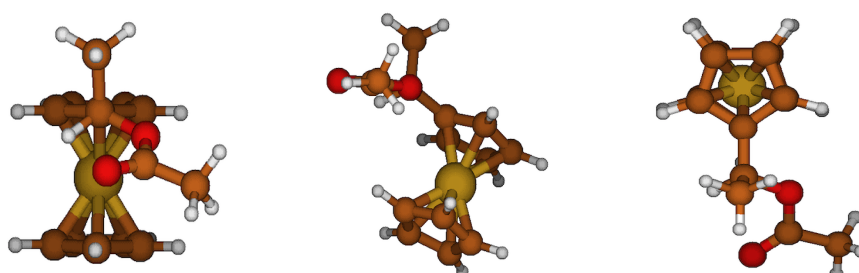


Figure SI 3: conformer III

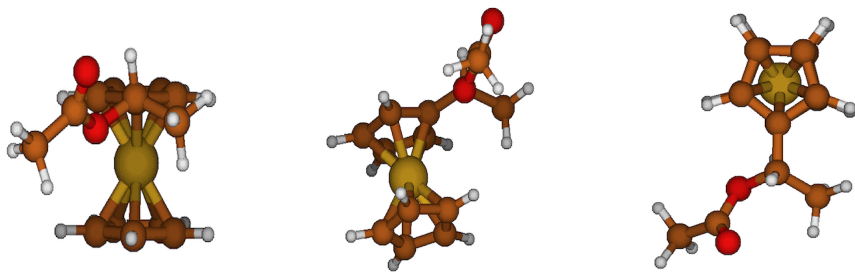


Figure SI 4: conformer IV

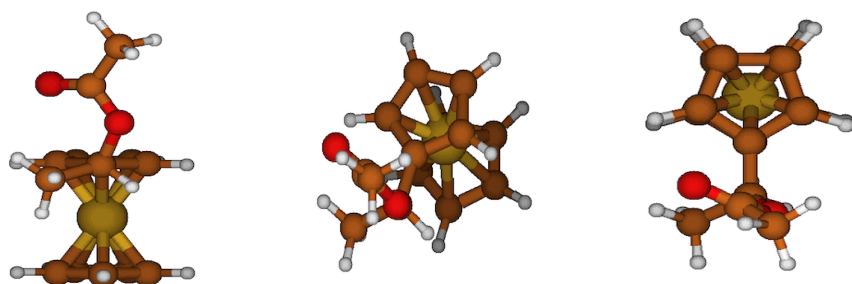


Figure SI 5: conformer V

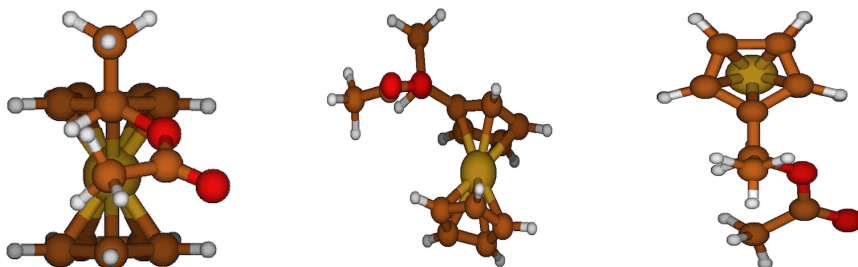


Figure SI 6: conformer VI

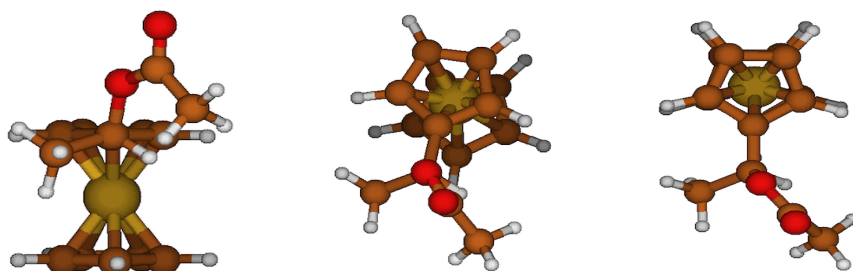


Figure SI 7: conformer VII

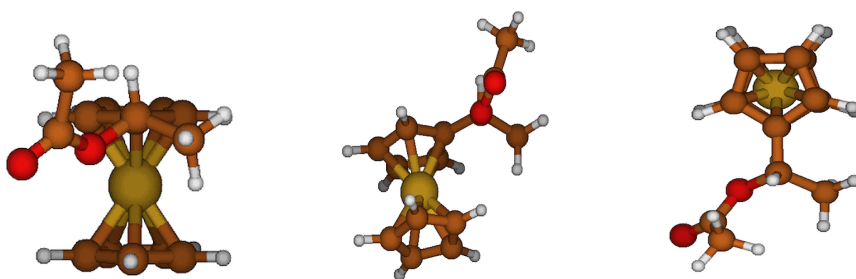


Figure SI 8: conformer VIII

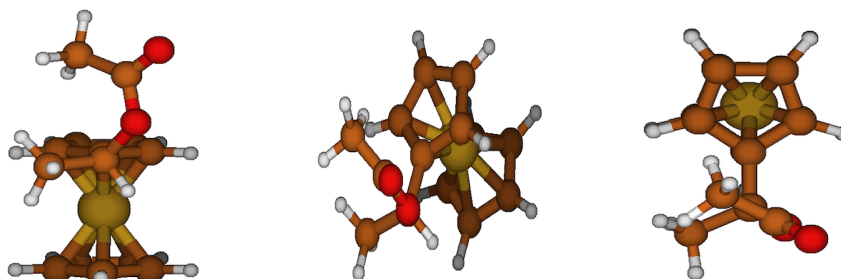


Figure SI 9: conformer IX

1.2 Assignment of normal modes of the most abundant conformer (T=298K)

conf. 1			conf. 1					
index	E(cm^{-1})	D($10^{-40}esu^2cm^2$)	R($10^{-44}esu^2cm^2$)	index	E(cm^{-1})	D($10^{-40}esu^2cm^2$)	R($10^{-44}esu^2cm^2$)	description
1	23.18	65.1	0.45	48	1045.83	169.37	-40.41	in plane bendings of CH (sCp ¹)
2	33.62	68.04	4.47	49	1058.98	23.86	1.30	bending of sMg ³
3	42.47	279.06	5.27	50	1061.91	245.78	54.35	in plane bendings of CH (sCp ¹) + bending of fMg ⁴ + stretching of C [*] —O(not of the carbonyl)
4	48.71	46.85	-12.30	51	1065.60	41.55	-2.25	in plane bendings of CH (bCp ⁵)
5	65.68	52.55	3.38	52	1069.91	16.51	-3.48	in plane bendings of CH (uCp ²)
6	96.28	45.64	-3.11	53	1072.20	61.56	-2.28	in plane bendings of CH (bCp ⁵)
7	165.71	28.27	0.50	54	1082.39	153.3	-18.93	in plane bendings of CH (sCp ¹) + bending of C [*] —H + bending of fMg ⁴
8	180.83	109.8	-2.01	55	1139.07	39.18	-29.40	in plane bendings of CH (sCp ¹) + stretching of C [*] —C(fMg ⁴)
9	191.20	86.38	1.80	56	1142.93	59.75	1.44	breathing (uCp ²)
10	230.16	28.46	3.37	57	1233.66	1.12	-10.04	in plane bendings of CH (sCp ¹) + bending of C [*] —H + bending of fMg
11	243.67	72.21	8.60	58	1263.49	1215.1	132.05	in plane bendings of CH (sCp ¹) + bending of C [*] —H + stretching of O(not of the carbonyl)—C(of the carbonyl)
12	255.22	37.41	24.43	59	1276.00	437.8	-34.68	in plane bendings of CH (sCp ¹) + bending of C [*] —H + stretching of O(not of the carbonyl)—C(of the carbonyl)
13	307.12	4.17	-0.68	60	1278.72	0.08	1.17	in plane and in phase bendings of CH (uCp ²)
14	321.99	3.53	2.16	61	1342.79	61.15	51.59	mainly bending of C [*] —H
15	379.21	11.05	2.58	62	1348.10	34.73	-8.88	C—C stretchings and in plane bendings of CH (sCp ¹) + bending of C [*] —H
16	404.18	12.36	1.07	63	1390.20	280.29	38.34	in phase bending of bMg ⁶ (mainly sMg ³)
17	454.75	254.04	-44.86	64	1393.45	18.43	-8.32	C—C stretchings and in plane bendings of CH (bCp ⁵) + bending of C [*] —H + in phase bending of bMg ⁶
18	473.83	209.48	7.37	65	1396.01	3.43	-3.52	C—C stretchings and in plane bendings of CH (mainly uCp ²) + bending of C [*] —H
19	483.23	197.61	10.08	66	1400.35	26.76	17.14	in phase bending of fMg ⁴
20	515.75	159.22	38.17	67	1413.87	10.88	4.03	C—C stretchings and in plane bendings of CH (bCp ⁵) + bending of C [*] —H + in phase bending of fMg ⁴
21	524.55	151.88	-30.90	68	1420.90	9.2	6.04	C—C stretchings and in plane bendings of CH (sCp ¹) + bending of C [*] —H
22	602.12	35.76	-3.00	69	1444.25	14.87	-18.30	C—C stretchings and in plane bendings of CH (uCp ²)
23	610.45	1.25	0.19	70	1453.81	1.92	-0.69	C—C stretchings and in plane bendings of CH (uCp ²)
24	612.30	0.34	0.11	71	1453.99	2.24	0.05	C—C stretchings and in plane bendings of CH (uCp ²)
25	614.96	2.47	-0.12	72	1456.31	52.49	2.58	bendings of sMg ³
26	625.24	37.44	-10.38	73	1464.42	36.05	-3.63	bendings of sMg ³
27	668.71	6.88	11.08	74	1476.00	18.0	-5.30	bendings of fMg ⁴
28	732.93	91.4	-23.18	75	1489.23	11.92	5.59	bendings of fMg ⁴
29	823.38	25.79	8.50	76	1510.71	5.16	-9.97	C—C stretchings and in plane bendings of CH (sCp ¹) + C [*] —C(sCp ¹) stretching + bendings of CH (fMg ⁴)
30	831.10	30.47	-8.35	77	1784.19	664.06	-48.21	carbonyl group stretching
31	835.24	244.09	-3.64	78	3056.16	22.49	-3.41	in phase CH stretchings (fMg ⁴)
32	840.55	38.21	1.69	79	3062.58	2.05	-0.14	in phase CH stretchings (sMg ³)
33	842.80	112.35	6.93	80	3100.20	6.03	11.80	C [*] —H stretching
34	845.97	16.29	1.59	81	3131.63	25.4	-4.04	CH stretchings (fMg ⁴)
35	848.25	80.47	-3.49	82	3132.36	6.26	3.18	CH stretchings (sMg ³)
36	856.85	22.51	-0.30	83	3140.76	27.22	-0.39	CH stretchings (fMg ⁴)
37	858.88	1.95	-0.47	84	3174.16	9.66	-0.42	CH stretchings (sMg ³)
38	886.27	14.74	2.14	85	3230.58	0.35	0.22	CH stretchings (bCp ⁵)
39	909.36	1.38	-0.35	86	3231.32	0.29	0.33	CH stretchings (bCp ⁵)
40	911.30	0.98	-0.45	87	3232.37	0.71	-0.31	CH stretchings (bCp ⁵)
41	915.26	1.28	-0.16	88	3240.06	4.75	-1.06	CH stretchings (sCp ¹)
42	924.36	45.7	1.46	89	3245.27	13.07	-2.15	CH stretchings (uCp ²)
43	962.82	87.58	-7.66	90	3246.10	7.57	2.24	CH stretchings (uCp ²)
44	1015.75	8.23	3.11	91	3248.64	6.39	-0.42	CH stretchings (sCp ¹)
45	1022.64	43.81	3.50	92	3254.90	4.09	-0.06	in phase CH stretchings (sCp ¹)
46	1023.98	29.78	7.62	93	3257.29	1.75	-0.11	in phase CH stretchings (uCp ²)
47	1030.30	443.48	31.09					mainly bending of sMg ³

Table SI 1: Normal mode assignment. Level of theory: B3PW91/Def2TZVP

¹ sCp stands for "substituted cyclopentadienyl moiety"

² uCp stands for "unsubstituted cyclopentadienyl moiety"

³ sMg stands for "second methyl group", namely the methyl group directly bounded to the carbonyl group

⁴ fMg stands for "first methyl group", namely the methyl group directly bounded to the chiral center C^{*}

⁵ bCp stands for "both cyclopentadienyl moieties"

⁶ bMg stands for "both methyl groups"

1.3 Anharmonic calculations: frozen LAMs and added Fermi resonances

Anharmonic calculations have been performed for the four most populated conformers. In what follows frozen LAMs and manually added (intensity-specific) Fermi resonances are listed for each conformer. All anharmonic energy derivatives involving at least 1 frozen LAM are nullified. The Fermi resonances are added to the set automatically built by analysis of the energy.

conformer	normal modes			Frozen LAMs	conformer	normal modes			Frozen LAMs
	i	j	k			i	j	k	
conf. I	47	9	32	3, 4, 5, 10	conf. III	45	20	20	1, 2, 3, 4, 10, 12
	47	16	26			61	13	48	
	51	17	23			65	19	39	
	54	11	33			72	19	43	
	55	21	25			72	21	42	
	58	14	43			77	15	67	
	58	15	38		conf. IV	42	13	23	1, 2, 3, 4, 11
	58	16	36			47	16	27	
	58	21	28			48	13	28	
	58	22	27			52	10	37	
	59	9	54			52	17	26	
	61	23	28			53	10	37	
	73	26	32			53	17	26	
	73	26	33			54	9	40	
conf. II	47	13	28	1, 2, 3, 5, 11	conf. IV	57	15	37	1, 2, 3, 4, 11
	48	10	29			58	12	43	
	53	10	34			58	22	27	
	55	4	54			59	10	49	
	59	9	54			59	12	43	
	59	10	48			59	13	43	
	59	13	43			59	16	38	
	59	17	29			59	24	27	
	60	22	27			59	26	27	
	69	15	50			60	13	43	
	72	22	34			64	14	47	
	73	25	34			66	14	48	
	73	26	33			67	19	41	
	74	26	37			73	26	33	
	77	20	58			73	26	34	
	77	20	59			75	18	44	
			77	20	59				
			77	28	49				
			77	29	43				

Table SI 2: manually added Fermi resonances ($\omega_i \approx \omega_j + \omega_k$) and frozen LAMs for each of the most populated conformers of 1-acetoxyethylferrocene. Level of theory: B3PW91/Def2TZVP

1.4 Calculated IR and VCD spectra of each conformer

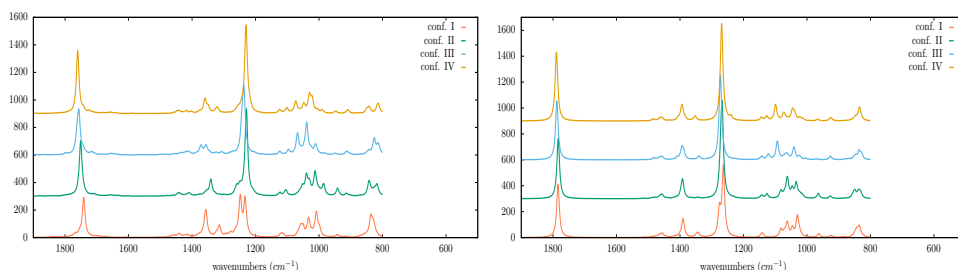


Figure SI 10: comparison between calculated anharmonic (figure on the left) and harmonic (figure on the right) mid-IR spectra for each of the most populated conformers; level of theory: B3PW91/Def2TZVP; intensity reported as molar absorption coefficient ϵ (dm³ mol⁻¹ cm⁻¹)

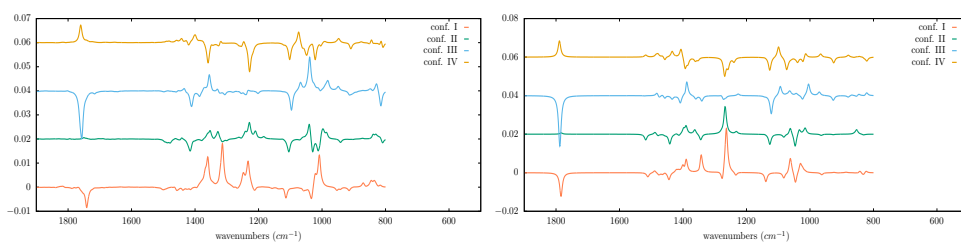


Figure SI 11: comparison between calculated anharmonic (figure on the left) and harmonic (figure on the right) mid-IR VCD spectra for each of the most populated conformers; level of theory: B3PW91/Def2TZVP; intensity reported as difference of molar absorption coefficients $\Delta\epsilon$ (dm³ mol⁻¹ cm⁻¹)

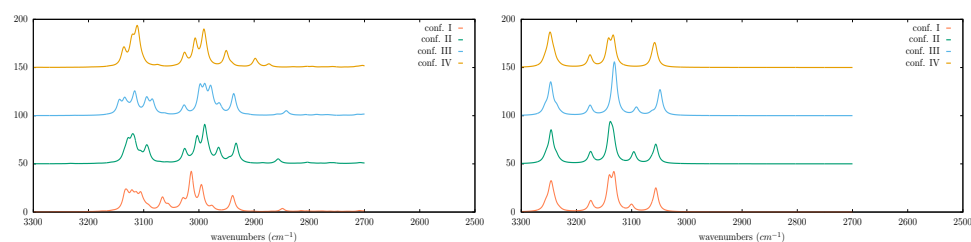


Figure SI 12: comparison between calculated anharmonic (figure on the left) and harmonic (figure on the right) IR spectra for each of the most populated conformers in the CH stretchings region; level of theory: B3PW91/Def2TZVP; intensity reported as molar absorption coefficient ϵ (dm³ mol⁻¹ cm⁻¹)

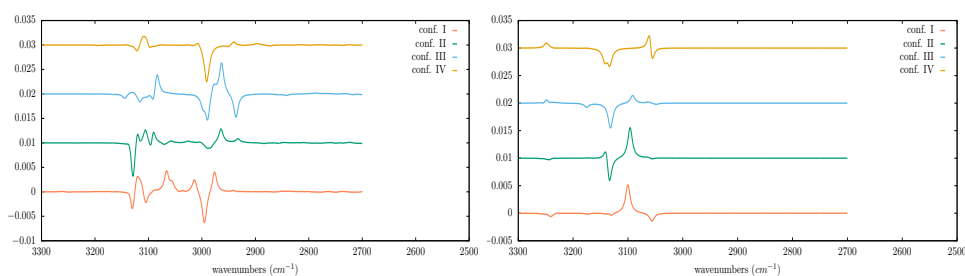


Figure SI 13: comparison between calculated anharmonic (figure on the left) and harmonic (figure on the right) VCD spectra for each of the most populated conformers in the CH stretchings region; level of theory: B3PW91/Def2TZVP; intensity reported as difference of molar absorption coefficients $\Delta\epsilon$ ($\text{dm}^3 \text{mol}^{-1} \text{cm}^{-1}$)

1.5 Experimental ^1H NMR spectrum and assignment

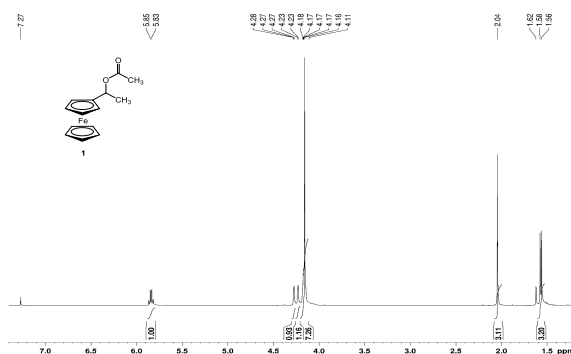


Figure SI 14: Experimental ^1H NMR spectrum of S-1-acetoxyethylferrocene

^1H -NMR (400 MHz, CDCl_3): δ 1.56 (3H, d, $J = 6.4$ Hz, CH_3), 2.04 (3H, s, COCH_3), 4.16 (7H, br s, Cp-H and $\text{Cp}'\text{-H}$), 4.23-4.27 (2H, d, o-Cp-H), 5.83-5.85 (1H, q, $\text{C}^*\text{-H}$).

1.6 coefficient of optical rotation: experimental values

$[\alpha]_D = +42.6$ (c 0.35, CHCl_3) for S -enantiomer, ee 95% (by chiral HPLC of the corresponding alcohol)

$[\alpha]_D = +23.8$ (c 0.35, EtOH) for S -enantiomer, ee 95% (by chiral HPLC of the corresponding alcohol)

Reference (T. Kijima, Y. Yaginuma, T. Izumi, *J. Chem. Technol. Biotechnol.*, 1999, **74**, 501-508): $[\alpha]_D = -27.1$ (c 0.85, EtOH) for R -enantiomer, ee 99%

2 S-1-methoxyethylferrocene

2.1 Structure of each conformer

In this section the structure of each conformer from different perspectives is reported; each geometry is optimized at the B3PW91/Def2TZVP level of theory.

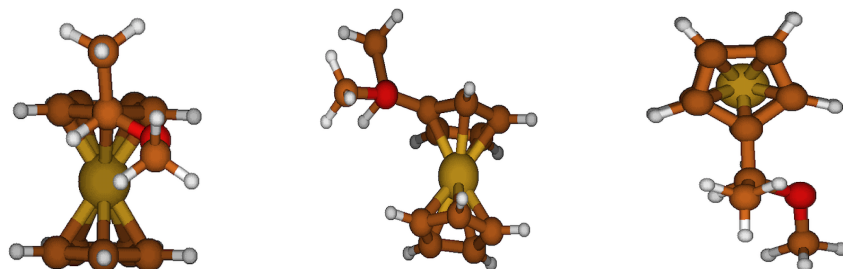


Figure SI 15: conformer I

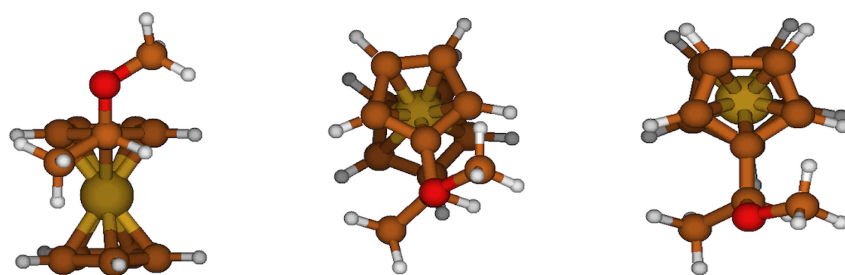


Figure SI 16: conformer II

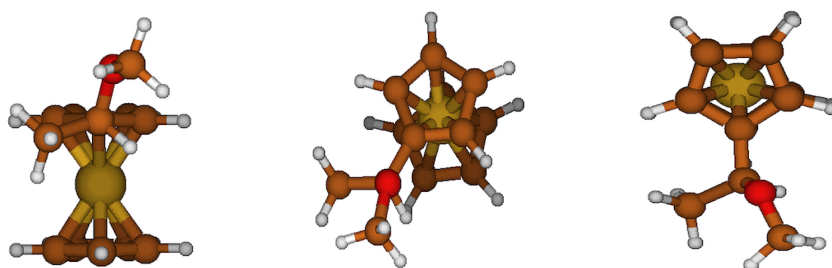


Figure SI 17: conformer III

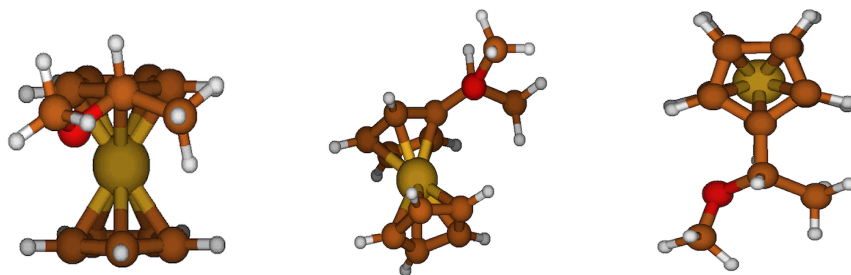


Figure SI 18: conformer IV

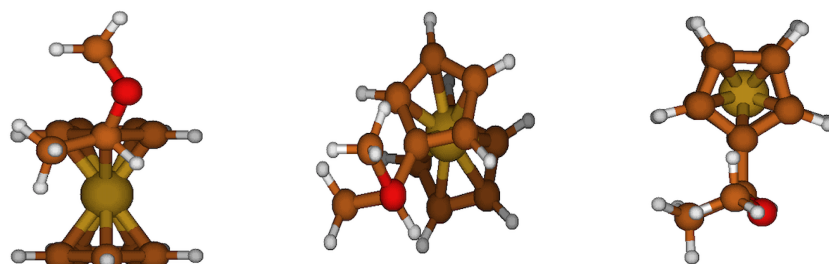


Figure SI 19: conformer V

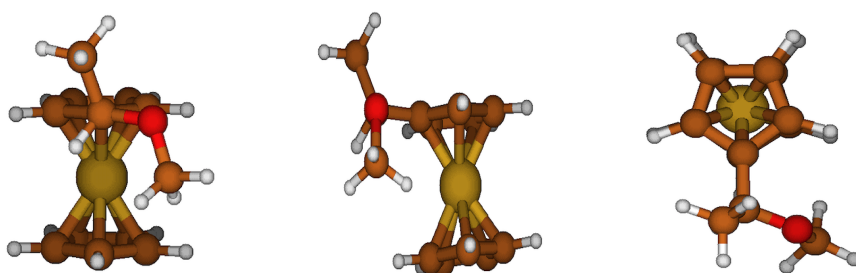


Figure SI 20: conformer VI

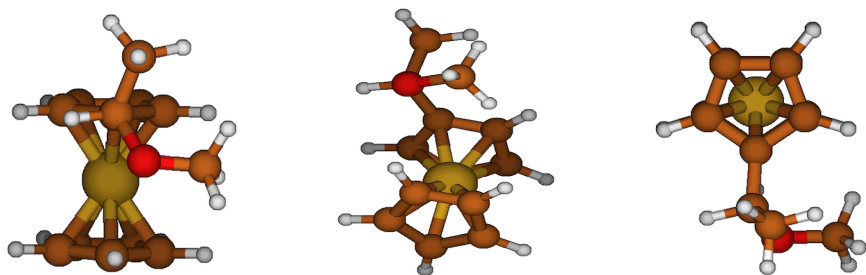


Figure SI 21: conformer VII

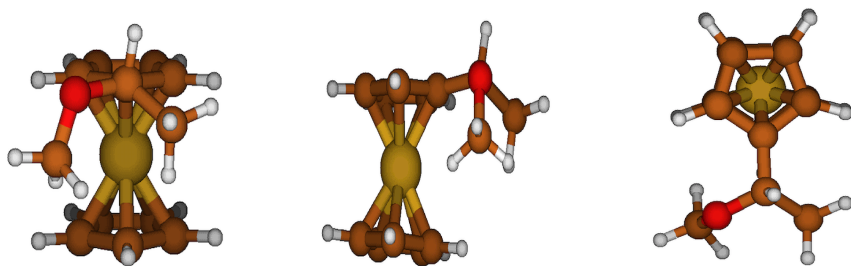


Figure SI 22: conformer VIII

2.2 Assignment of normal modes of the most abundant conformer (T=298K)

conf. 1			conf. 1						
index	$E(\text{cm}^{-1})$	$D(10^{-40}\text{esu}^2\text{cm}^2)$	$R(10^{-44}\text{esu}^2\text{cm}^2)$	description	index	$E(\text{cm}^{-1})$	$D(10^{-40}\text{esu}^2\text{cm}^2)$	$R(10^{-44}\text{esu}^2\text{cm}^2)$	description
1	32.27	3.19	-1.54	hindered rotation of $\text{C}^*-\text{C}(\text{sCp}^1)-\text{Fe}-\text{C}(\text{uCp}^2)$	45	1068.89	1.2	-0.24	in plane bendings of CH (uCp ²)
2	37.73	33.02	2.29	hindered rotation of $\text{Fe}-\text{C}(\text{sCp}^1)-\text{C}^*-\text{O}$	46	1070.95	2.11	4.53	in plane bendings of CH (bCp ²)
3	55.72	176.89	-4.08	mainly hindered rotation of sMg^3	47	1082.77	10.05	-0.3	in plane bendings of CH (sCp ¹) + bending of C^*-H + bending of fMg^5
4	88.90	70.95	-3.66	mainly hindered rotation of sMg^3	48	1103.47	25.64	31.37	stretching of $\text{C}^*-\text{C}(\text{fMg}^5)$
5	151.55	30.79	-0.99	hindered rotation of $\text{C}^*-\text{C}(\text{sCp}^1)-\text{Fe}-\text{C}(\text{uCp}^2)$	49	1142.44	65.29	0.10	breathing (uCp ²)
6	167.16	27.49	-0.41	hindered rotation of sMg^3 + bending of $\text{uCp}^2-\text{Fe}-\text{sCp}^1$	50	1151.55	630.91	-36.69	stretchings of C^*-O and $\text{O}-\text{C}(\text{sMg}^3)$
7	181.35	39.55	-4.71	mainly hindered rotation of sMg^3	51	1171.79	10.35	2.52	bending of sMg^3
8	204.13	14.47	-9.89	mainly hindered rotation of bMg^4	52	1205.92	170.38	9.69	in plane bendings of CH (sCp ¹) + bending of C^*-H + bending of sMg^3
9	242.05	23.92	-6.10	mainly hindered rotation of fMg^5	53	1235.95	30.86	5.18	in plane bendings of CH (sCp ¹) + bending of C^*-H + bending of sMg^3
10	262.56	4.3	6.84	mainly hindered rotation of fMg^5	54	1262.11	24.65	-12.52	in plane bendings of CH (sCp ¹) + bending of C^*-H + stretching of $\text{C}^*-\text{C}(\text{sCp}^1)$
11	307.76	6.59	3.31	skeletal deformations (whole molecule), Fe atom not involved	55	1277.39	0.01	0.12	in plane and in phase bendings of CH (uCp ²)
12	332.45	22.68	10.12	bending of $\text{C}^*-\text{O}-\text{C}(\text{sMg}^3)$	56	1339.89	72.01	2.21	mainly bending of C^*-H
13	367.28	14.91	0.36	skeletal deformations (whole molecule), Fe atom not involved	57	1356.98	63.14	-47.90	mainly bending of C^*-H
14	393.68	36.62	17.55	skeletal deformations (whole molecule), Fe atom not involved	58	1387.10	45.06	-14.61	in phase bending of fMg^5
15	428.26	39.52	14.24	skeletal deformations (whole molecule), Fe atom involved	59	1391.45	6.99	4.72	$\text{C}-\text{C}$ stretchings and in plane bendings of CH (bCp ²) + bending of C^*-H
16	472.70	221.5	-33.77	skeletal deformations (whole molecule), Fe atom involved	60	1395.58	2.72	-0.42	$\text{C}-\text{C}$ stretchings and in plane bendings of CH (mainly uCp ²) + bending of C^*-H
17	487.18	168.37	26.64	uCp^2-Fe and $\text{Fe}-\text{sCp}^1$ stretchings	61	1408.03	6.15	2.31	$\text{C}-\text{C}$ stretchings and in plane bendings of CH (bCp ²) + bending of C^*-H
18	509.29	251.89	-8.50	skeletal deformations (whole molecule), Fe atom involved	62	1421.64	4.76	-3.69	$\text{C}-\text{C}$ stretchings and in plane bendings of CH (mainly sCp ¹) + bending of C^*-H
19	523.34	172.04	-9.72	skeletal deformations (whole molecule), Fe atom involved	63	1433.04	8.38	19.96	$\text{C}-\text{C}$ stretchings and in plane bendings of CH (sCp ¹) + bending of C^*-H
20	610.25	0.22	-0.12	out of plane deformations (bCp ²)	64	1452.82	1.77	-1.19	$\text{C}-\text{C}$ stretchings and in plane bendings of CH (uCp ²)
21	612.10	0.05	-0.05	out of plane deformations (uCp ²)	65	1453.25	1.54	-0.21	$\text{C}-\text{C}$ stretchings and in plane bendings of CH (uCp ²)
22	614.40	0.03	<-0.01	out of plane deformations (bCp ²)	66	1464.70	5.95	2.51	in phase bending of sMg^3 + bending of fMg^5
23	675.90	8.99	-6.60	bending of $\text{Fe}-\text{C}(\text{sCp}^1)-\text{C}^*$	67	1470.99	22.04	-13.66	bendings of bMg^4
24	715.47	1.52	-1.76	bendings of $\text{Fe}-\text{C}(\text{sCp}^1)-\text{C}^*$ and $\text{C}(\text{sCp}^1)-\text{C}^*-\text{C}(\text{fMg}^5)$	68	1476.66	5.98	-1.39	bendings of bMg^4
25	820.27	4.75	7.41	out of plane bendings of CH (bCp ²)	69	1490.91	14.58	14.02	bendings of bMg^4
26	825.16	37.23	7.84	out of plane bendings of CH (bCp ²)	70	1499.42	26.91	19.45	bending of sMg^3
27	831.18	330.13	-2.72	in phase out of plane bendings of CH (uCp ²)	71	1521.67	1.36	-2.01	$\text{C}-\text{C}$ stretchings and in plane bendings of CH (sCp ¹) + $\text{C}^*-\text{C}(\text{sCp}^1)$ stretching + bendings of CH (methoxyethyl group)
28	840.74	0.47	0.28	in plane ring deformations (bCp ²) + out of plane bendings of CH (bCp ²)	72	2970.47	44.28	-43.96	C^*-H stretching
29	843.93	59.84	-0.31	out of plane bendings of CH (bCp ²)	73	2985.63	106.85	13.33	in phase CH stretchings (sMg ³)
30	845.72	2.88	-0.24	in plane ring deformations (uCp ²) + out of plane bendings of CH (uCp ²)	74	3039.83	35.31	-64.58	in phase CH stretchings (fMg ⁵) + CH stretchings (sMg ³)
31	852.78	47.19	-0.28	out of plane bendings of CH (bCp ²)	75	3046.56	82.94	23.67	in phase CH stretchings (fMg ⁵) + CH stretchings (sMg ³)
32	858.48	3.26	1.55	in plane ring deformations (bCp ²) + out of plane bendings of CH (bCp ²)	76	3119.16	45.1	42.59	CH stretchings (fMg ⁵) + CH stretchings (sMg ³)
33	863.16	11.22	1.19	out of plane bendings of CH (bCp ²) + bendings of C^*H and fMg^5	77	3121.92	33.0	-27.96	CH stretchings (fMg ⁵) + CH stretchings (sMg ³)
34	880.72	26.35	-5.24	out of plane bendings of CH (bCp ²)	78	3125.53	27.97	-3.72	CH stretchings (fMg ⁵)
35	905.35	0.12	0.08	out of plane bendings of CH (bCp ²)	79	3226.42	1.46	0.08	CH stretchings (sCp ¹)
36	906.79	1.37	-0.15	out of plane bendings of CH (bCp ²)	80	3230.07	0.22	0.12	CH stretchings (uCp ²)
37	910.33	0.1	-0.09	out of plane bendings of CH (bCp ²)	81	3232.86	0.04	0.05	CH stretchings (uCp ²)
38	932.23	83.43	-27.30	in plane ring deformation and in plane bending of CH (sCp ¹) + bending of fMg^5	82	3234.70	7.7	0.15	CH stretchings (sCp ¹)
39	1012.85	72.27	36.73	in plane bendings of CH (bCp ²) + bending of C^*-H + bending of bMg^4	83	3245.39	9.72	-5.81	CH stretchings (uCp ²)
40	1021.91	37.48	-0.47	in plane bendings of CH (uCp ²)	84	3246.67	4.33	12.22	CH stretchings (bCp ²)
41	1022.98	48.7	-17.04	in plane bendings of CH (uCp ²)	85	3247.14	18.93	-6.05	CH stretchings (bCp ²)
42	1040.35	59.77	14.33	in plane bendings of CH (uCp ²)	86	3257.82	4.17	-0.38	in phase CH stretchings (bCp ²)
43	1056.52	36.23	25.06	in plane bendings of CH (sCp ¹) + bending of fMg^5	87	3258.26	1.49	0.38	in phase CH stretchings (bCp ²)
44	1063.20	3.49	5.61	in plane bendings of CH (bCp ²)					

Table SI 3: Normal mode assignment. Level of theory: B3PW91/Def2TZVP

¹ sCp stands for "substituted cyclopentadienyl moiety"

² uCp stands for "unsubstituted cyclopentadienyl moiety"

³ sMg stands for "second methyl group", namely the methyl group directly bounded to the oxygen

⁴ bMg stands for "both methyl groups"

⁵ fMg stands for "first methyl group", namely the methyl group directly bounded to the chiral center C^*

⁶ bCp stands for "both cyclopentadienyl moieties"

2.3 Anharmonic calculations: frozen LAMs and added Fermi resonances

Anharmonic calculations have been performed for the five most populated conformers. In what follows frozen LAMs and manually added (intensity-specific) Fermi resonances are listed for each conformer. All anharmonic energy derivatives involving at least 1 frozen LAM are nullified. The Fermi resonances are added to the set automatically built by analysis of the energy.

conformer	normal modes			Frozen LAMs	conformer	normal modes			Frozen LAMs
	i	j	k			i	j	k	
conf. I	39	5	33	2, 3, 4, 7, 8	conf. III	59	18	34	1, 2, 3, 7, 8, 10
	39	17	19			61	12	47	
	42	15	22			61	14	39	
	57	15	38			70	16	39	
	69	5	56			70	23	31	
	69	15	44			72	66	71	
	70	10	53			72	67	70	
	70	15	46			73	66	71	
	70	17	39			73	67	70	
	72	66	69			78	4	75	
72	67	69		39	18	19			
75	71	71		42	15	22			
conf. II	40	17	19	4, 7, 9	conf. IV	47	16	21	1, 3, 5, 8, 9
	42	18	19			49	10	32	
	43	8	30			50	4	43	
	48	10	33			50	4	44	
	50	11	29			50	19	23	
	50	11	30			52	12	33	
	50	11	31			52	13	32	
	51	15	24			56	15	38	
	53	3	50			57	12	39	
	56	10	47			57	17	32	
	56	18	25			57	23	24	
	56	20	24			59	11	45	
	58	16	37			59	12	42	
	61	12	43			69	16	39	
62	17	38	69	16	40				
63	21	26	73	66	71				
69	23	29	73	67	70				
72	66	70	77	7	72				
72	67	70		40	16	19			
72	67	71		41	16	19			
72	68	70		43	15	20			
73	68	71		47	6	37			
73	69	70		47	12	24			
conf. III	49	14	24	1, 2, 3, 7, 8, 10	conf. V	49	8	38	3, 4, 5, 9, 10
	54	12	38			50	2	48	
	54	19	24			50	8	38	
	56	19	25			50	11	28	
	56	20	24			54	7	46	
	57	16	34			54	15	25	
	57	18	29			67	12	50	
	58	13	39			67	19	38	
58	13	41		72	70	71			

Table SI 4: manually added Fermi resonances ($\omega_i \approx \omega_j + \omega_k$) and frozen LAMs for each of the most populated conformers of 1-methoxyethylferrocene. Level of theory: B3PW91/Def2TZVP

2.4 Calculated IR and VCD spectra of each conformer

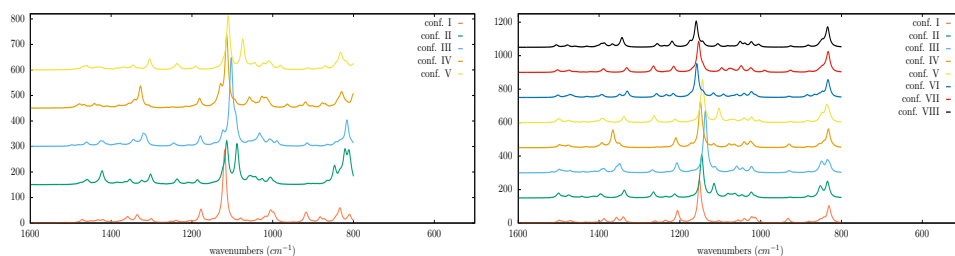


Figure SI 23: comparison between calculated anharmonic (figure on the left) and harmonic (figure on the right) mid-IR spectra for each conformer; level of theory: B3PW91/Def2TZVP; intensity reported as molar absorption coefficient ϵ ($\text{dm}^3 \text{mol}^{-1} \text{cm}^{-1}$)

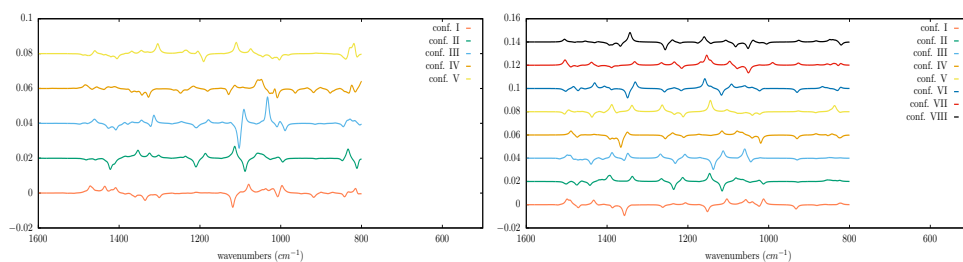


Figure SI 24: comparison between calculated anharmonic (figure on the left) and harmonic (figure on the right) mid-IR VCD spectra for each conformer; level of theory: B3PW91/Def2TZVP; intensity reported as difference of molar absorption coefficients $\Delta\epsilon$ ($\text{dm}^3 \text{mol}^{-1} \text{cm}^{-1}$)

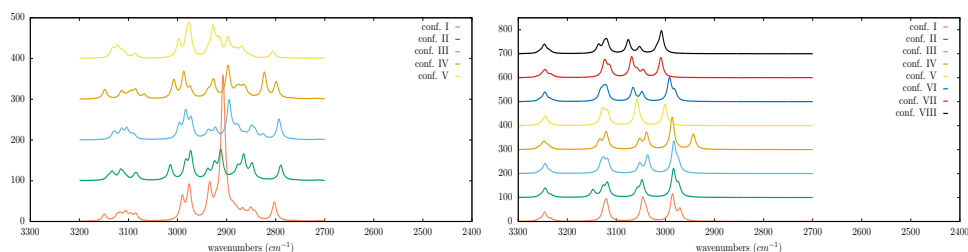


Figure SI 25: comparison between calculated anharmonic (figure on the left) and harmonic (figure on the right) IR spectra for each conformer in the CH stretchings region; level of theory: B3PW91/Def2TZVP; intensity reported as molar absorption coefficient ϵ ($\text{dm}^3 \text{mol}^{-1} \text{cm}^{-1}$)

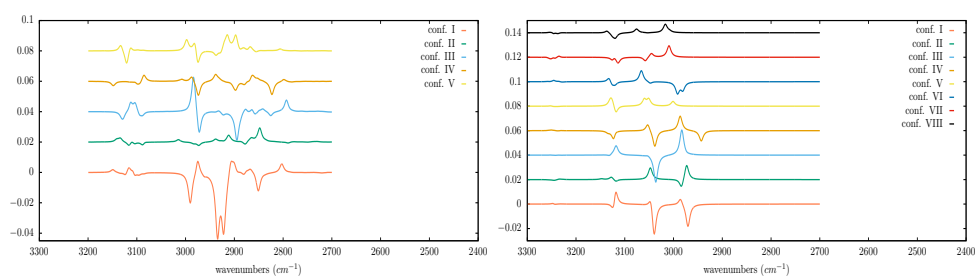


Figure SI 26: comparison between calculated anharmonic (figure on the left) and harmonic (figure on the right) VCD spectra for each conformer in the CH stretchings region; level of theory: B3PW91/Def2TZVP; intensity reported as difference of molar absorption coefficients $\Delta\epsilon$ ($\text{dm}^3 \text{mol}^{-1} \text{cm}^{-1}$)

2.5 Experimental and computational spectra in the 1500-1900 cm^{-1} region

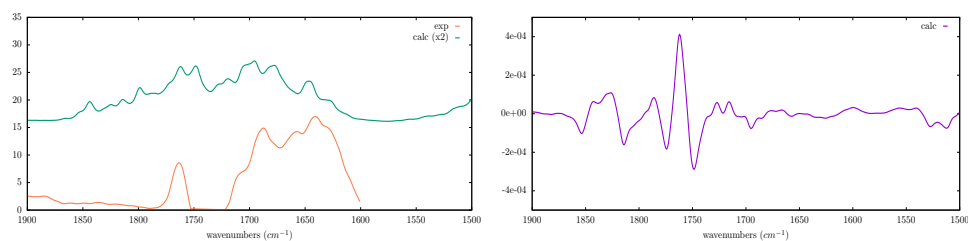


Figure SI 27: comparison between anharmonic and experimental IR spectra (figure on the left); anharmonic VCD spectrum (figure on the right); level of theory: B3PW91/Def2TZVP; intensity reported, respectively, as molar extinction coefficients ϵ and their differences $\Delta\epsilon$ ($\text{dm}^3 \text{mol}^{-1} \text{cm}^{-1}$)

2.6 Experimental ^1H NMR spectrum and assignment

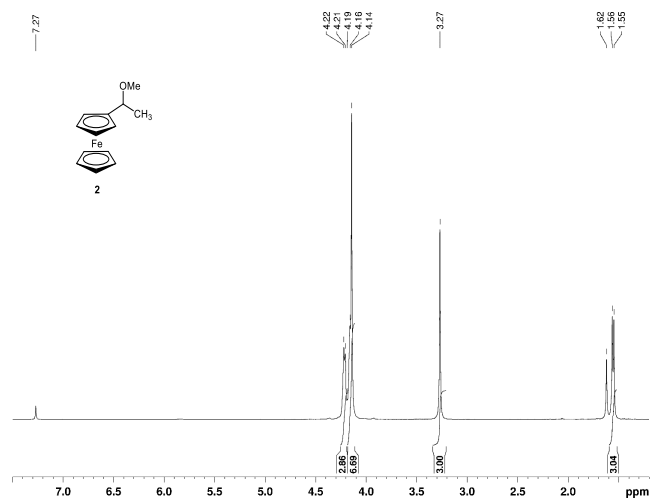


Figure SI 28: Experimental ^1H NMR spectrum of S-1-methoxyethylferrocene

^1H -NMR (400 MHz, CDCl_3): δ 1.56 (3H, d, $J = 6.4$ Hz, CH_3), 3.27 (3H, s, OMe), 4.16 (7H, br s, Cp—H and Cp'—H), 4.21 (3H, m, o-Cp—H and C*—H).

2.7 coefficient of optical rotation: experimental value

$[\alpha]_D = -17.9$ (c 0.39, CHCl_3) for *S*-enantiomer, *ee* 95% (by chiral HPLC of the corresponding alcohol)

Reference (P. Vicennati, P.G. Cozzi, *Eur. J. Org. Chem.*, 2007, 2248-2253):

$[\alpha]_D = -20.0$ (c 0.2, CHCl_3) for *S*-enantiomer, *ee* 86%

3 S-1-hydroxyethylferrocene

3.1 Structure of each conformer

In this section the structure of each conformer from different perspectives is reported; each geometry is optimized at the B3PW91/Def2TZVP level of theory.

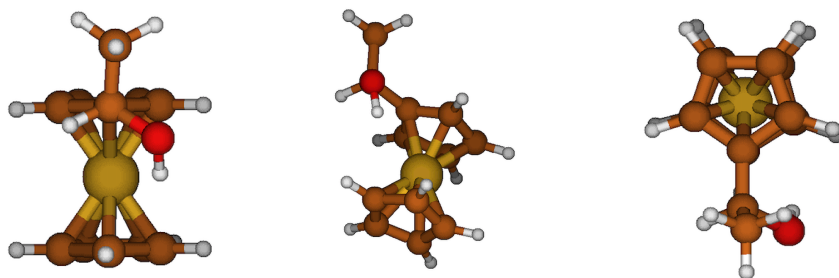


Figure SI 29: conformer I

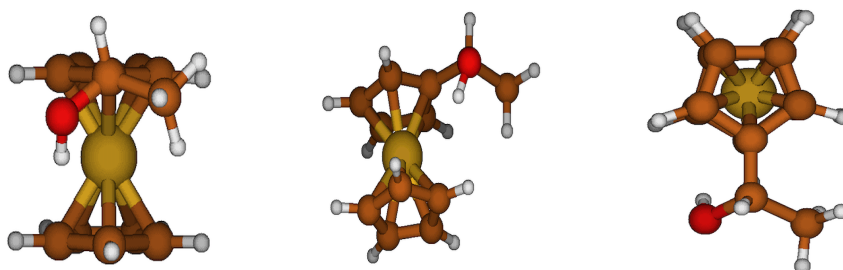


Figure SI 30: conformer II

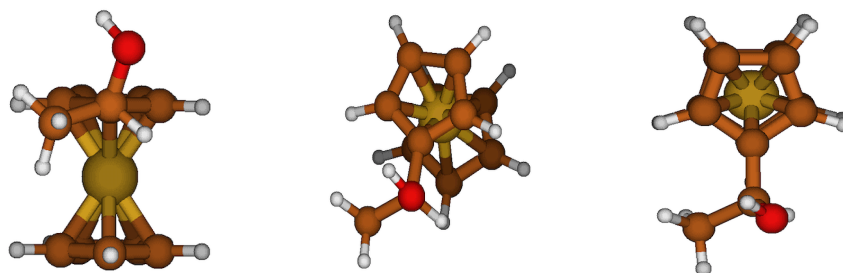


Figure SI 31: conformer III

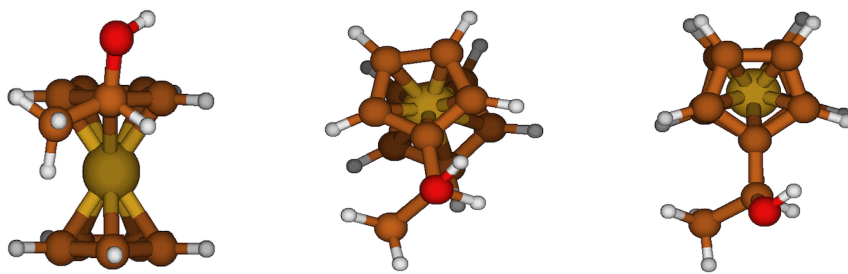


Figure SI 32: conformer IV

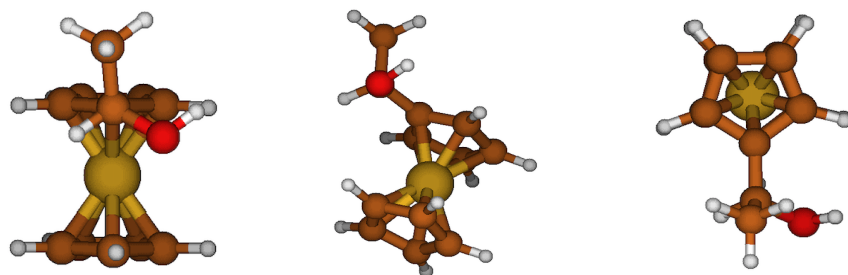


Figure SI 33: conformer V

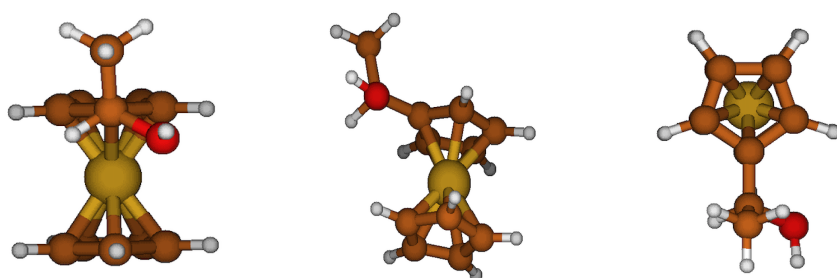


Figure SI 34: conformer VI

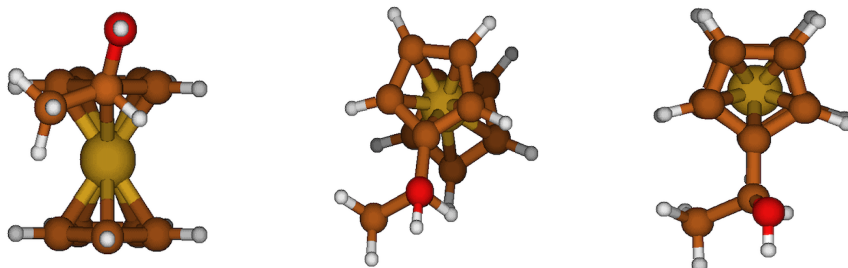


Figure SI 35: conformer VII

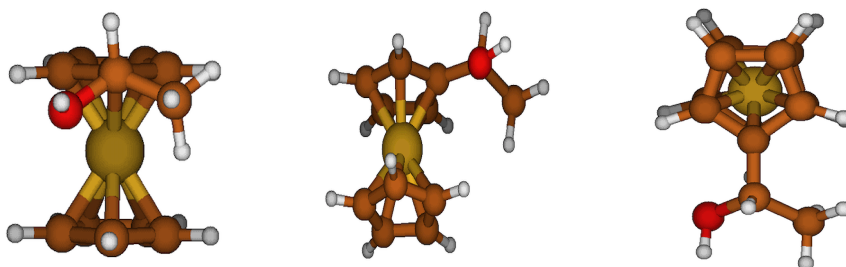


Figure SI 36: conformer VIII

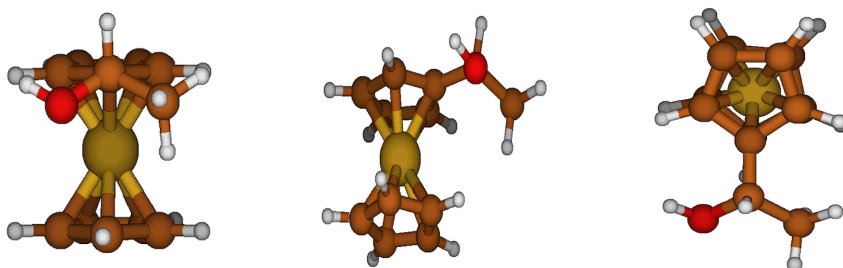


Figure SI 37: conformer IX

3.2 Assignment of normal modes of the most abundant conformer (T=298K)

conf. I				conf. I			
index	$E(\text{cm}^{-1})$	$D(10^{-40}\text{esu}^2\text{cm}^2)$	$R(10^{-44}\text{esu}^2\text{cm}^2)$	index	$E(\text{cm}^{-1})$	$D(10^{-40}\text{esu}^2\text{cm}^2)$	$R(10^{-44}\text{esu}^2\text{cm}^2)$
1	35.99	7.03	-2.68	40	1042.49	51.73	7.33
2	63.49	115.45	6.13	41	1060.04	12.20	-4.26
3	87.63	18.21	-1.26	42	1066.60	24.35	10.43
4	167.12	50.73	2.54	43	1071.59	4.12	0.78
5	175.54	28.79	-3.91	44	1072.55	40.09	24.33
6	201.31	18.13	-5.26	45	1078.64	51.70	33.10
7	247.36	3.58	3.38	46	1131.21	143.88	29.66
8	252.55	50.00	-9.99	47	1142.22	69.41	-9.79
9	304.99	77.16	1.79	48	1227.26	0.84	-1.75
10	351.60	521.72	-0.11	49	1253.50	62.74	-49.37
11	372.95	282.09	-59.06	50	1279.61	3.49	0.67
12	400.26	266.20	0.27	51	1282.96	132.08	-34.75
13	433.70	141.25	-8.48	52	1341.50	50.38	-2.70
14	475.41	96.80	1.78	53	1381.82	51.06	28.02
15	483.95	220.66	-15.65	54	1394.02	1.66	0.56
16	505.82	203.42	-3.80	55	1395.75	2.69	-0.10
17	525.85	248.64	-1.69	56	1406.41	106.29	16.41
18	610.11	0.06	-0.09	57	1412.64	12.45	3.17
19	612.31	0.77	-0.01	58	1423.47	28.08	-4.60
20	614.78	0.64	-0.04	59	1439.07	11.55	24.80
21	679.31	3.06	2.26	60	1453.30	3.20	0.87
22	690.78	8.32	-2.76	61	1454.40	2.28	0.83
23	825.00	1.67	7.13	62	1472.05	14.91	-11.52
24	831.89	178.05	-0.54	63	1481.86	14.57	7.79
25	837.62	120.79	-4.00	64	1513.38	5.66	12.61
26	841.83	7.79	-1.31	65	2980.91	65.05	-15.00
27	844.69	1.03	0.24	66	3045.76	34.88	1.59
28	850.61	116.50	-1.02	67	3123.85	36.01	-10.95
29	857.41	26.26	5.23	68	3128.29	27.02	8.75
30	859.05	2.98	-0.39	69	3224.21	1.42	0.88
31	885.10	14.73	2.62	70	3228.36	0.73	0.18
32	897.36	42.47	17.66	71	3231.89	0.12	-0.45
33	909.90	0.04	0.03	72	3235.11	5.00	-0.24
34	914.15	3.07	-1.30	73	3241.60	8.91	3.94
35	915.18	1.94	0.73	74	3244.77	4.50	-6.34
36	943.42	46.15	-25.66	75	3245.72	11.39	4.83
37	1011.56	158.50	0.98	76	3252.99	4.73	-1.15
38	1022.57	62.81	-6.69	77	3256.10	2.27	0.20
39	1024.90	33.77	-9.77	78	3791.01	55.84	12.03

Table SI 5: Normal mode assignment. Level of theory: B3PW91/Def2TZVP

- ¹ sCp stands for "substituted cyclopentadienyl moiety"
- ² uCp stands for "unsubstituted cyclopentadienyl moiety"
- ³ bCp stands for "both cyclopentadienyl moieties"

3.3 Anharmonic calculations: frozen LAMs and added Fermi resonances

Anharmonic calculations have been performed for the six most populated conformers. In what follows frozen LAMs and manually added (intensity-specific) Fermi resonances are listed for each conformer. All anharmonic energy derivatives involving at least 1 frozen LAM are nullified. The Fermi resonances are added to the set automatically built by analysis of the energy.

conformer	normal modes			Frozen LAMs	conformer	normal modes			Frozen LAMs
	i	j	k			i	j	k	
conf. I	37	15	17	1, 2, 7, 10, 11, 12	conf. IV	43	13	21	1, 2, 7, 8, 9, 10
	37	16	16			46	5	36	
	40	13	18			48	4	41	
	53	8	46			50	6	41	
conf. II	40	13	18	7, 9	50	12	32	1, 2, 7, 8, 9, 10	
	45	3	37		50	21	21		
	46	2	38		58	11	43		
	46	3	37		68	3	66		
	54	11	39		conf. V	41	5		31
56	4	48	46	5		36			
56	8	45	52	10		37			
56	12	38	52	21		21			
56	14	36	57	11		40			
conf. III	56	15	34	1, 2, 6, 7, 8, 9	57	12	37	1, 2, 7, 8, 9	
	56	17	31		59	17	33		
	57	17	31		46	5	36		
	37	12	21		53	17	29		
	41	17	17		53	22	22		
conf. VI	45	15	18	1, 2, 6, 7, 8, 9	59	12	40	1, 2, 7, 8, 9	
	55	12	37		62	6	50		
	56	17	31		63	6	50		
	57	17	31						

Table SI 6: manually added Fermi resonances ($\omega_i \approx \omega_j + \omega_k$) and frozen LAMs for each of the most populated conformers of 1-hydroxyethylferrocene. Level of theory: B3PW91/Def2TZVP

3.4 Calculated IR and VCD spectra of each conformer

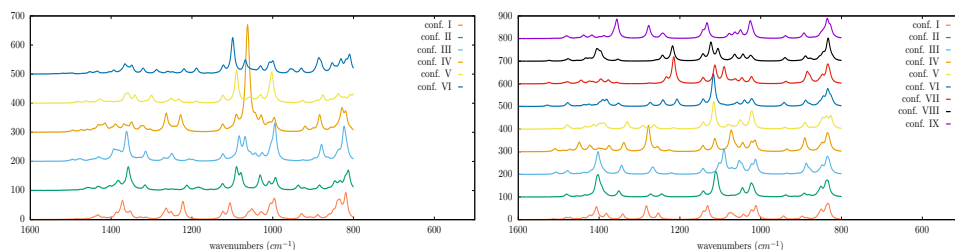


Figure SI 38: comparison between calculated anharmonic (figure on the left) and harmonic (figure on the right) mid-IR spectra for each conformer; level of theory: B3PW91/Def2TZVP; intensity reported as molar absorption coefficient ϵ ($\text{dm}^3 \text{mol}^{-1} \text{cm}^{-1}$)

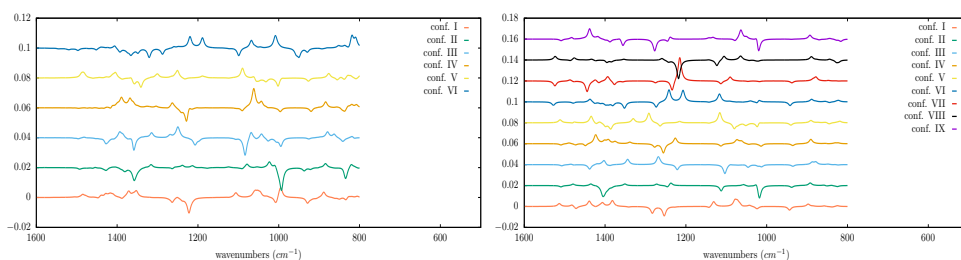


Figure SI 39: comparison between calculated anharmonic (figure on the left) and harmonic (figure on the right) mid-IR VCD spectra for each conformer; level of theory: B3PW91/Def2TZVP; intensity reported as difference of molar absorption coefficients $\Delta\epsilon$ ($\text{dm}^3 \text{mol}^{-1} \text{cm}^{-1}$)

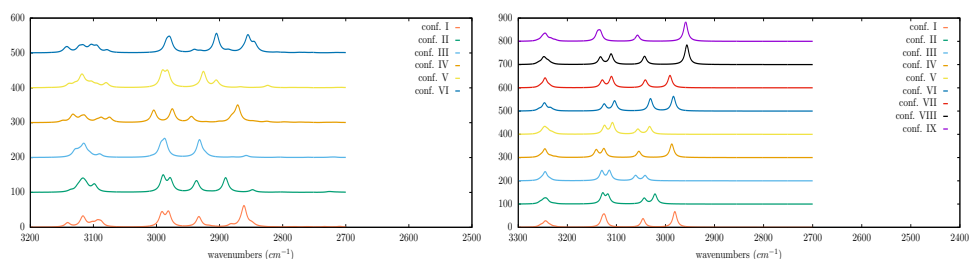


Figure SI 40: comparison between calculated anharmonic (figure on the left) and harmonic (figure on the right) IR spectra for each conformer in the CH stretchings region; level of theory: B3PW91/Def2TZVP; intensity reported as molar absorption coefficient ϵ ($\text{dm}^3 \text{mol}^{-1} \text{cm}^{-1}$)

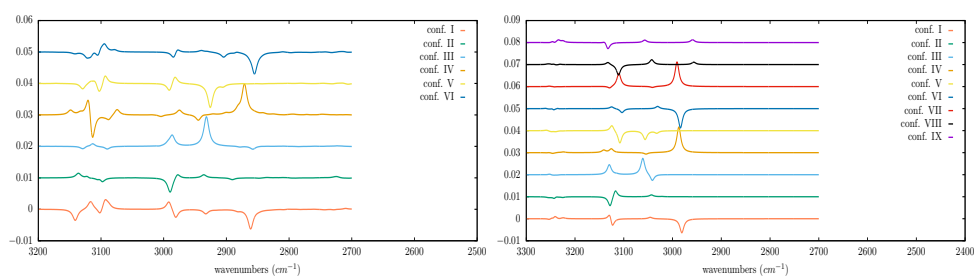


Figure SI 41: comparison between calculated anharmonic (figure on the left) and harmonic (figure on the right) VCD spectra for each conformer in the CH stretchings region; level of theory: B3PW91/Def2TZVP; intensity reported as difference of molar absorption coefficients $\Delta\epsilon$ ($\text{dm}^3 \text{mol}^{-1} \text{cm}^{-1}$)

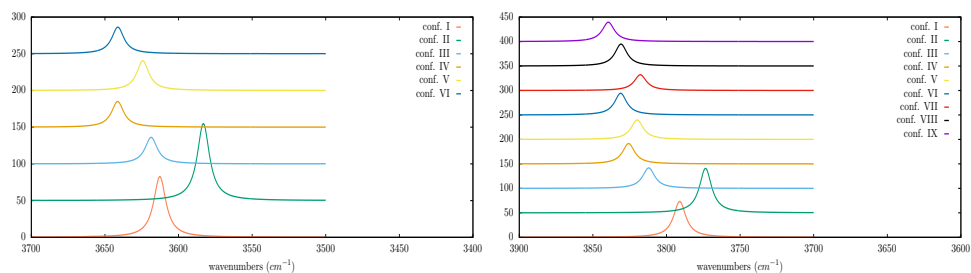


Figure SI 42: comparison between calculated anharmonic (figure on the left) and harmonic (figure on the right) IR spectra for each conformer in the OH stretchings region; level of theory: B3PW91/Def2TZVP; intensity reported as molar absorption coefficient ϵ ($\text{dm}^3 \text{mol}^{-1} \text{cm}^{-1}$)

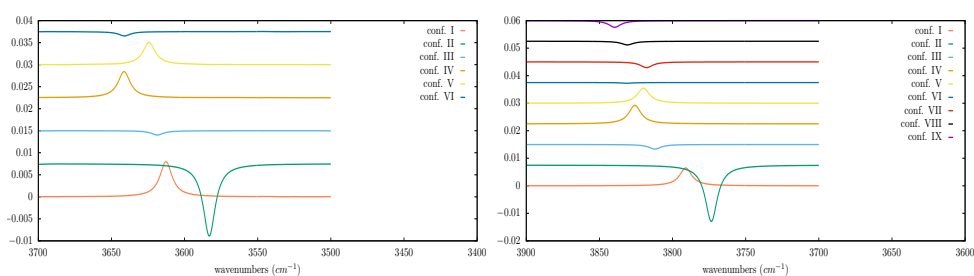


Figure SI 43: comparison between calculated anharmonic (figure on the left) and harmonic (figure on the right) VCD spectra for each conformer in the OH stretchings region; level of theory: B3PW91/Def2TZVP; intensity reported as difference of molar absorption coefficients $\Delta\epsilon$ ($\text{dm}^3 \text{mol}^{-1} \text{cm}^{-1}$)

3.5 Frequencies, IR intensities and rotational strength in the OH stretchings region for each conformer

conformer	OH stretchings		
	E(cm^{-1})	D($10^{-40} \text{esu}^2 \text{cm}^2$)	R($10^{-44} \text{esu}^2 \text{cm}^2$)
I	3791.01	55.84	12.03
II	3773.47	69.50	-38.08
III	3812.06	31.71	-3.06
IV	3825.71	31.41	12.34
V	3819.91	30.03	10.12
VI	3831.14	33.44	-0.46
VII	3817.76	24.31	-3.85
VIII	3830.90	33.74	-2.41
IX	3839.50	29.73	-4.45

Table SI 7: frequencies, IR intensities and rotational strengths of OH stretching for each conformer; level of theory: B3PW91/Def2TZVP

3.6 Experimental and computational spectra in the 1500-1900 cm^{-1} region

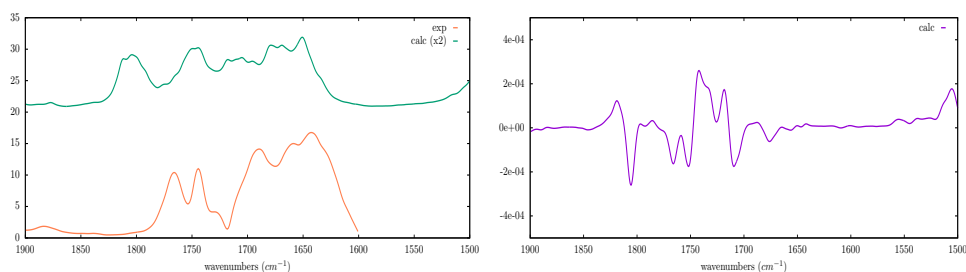


Figure SI 44: comparison between anharmonic spectrum and experimental IR spectra (figure on the left); anharmonic VCD spectrum (figure on the right); level of theory: B3PW91/Def2TZVP; intensity reported, respectively, as molar extinction coefficients ϵ and their differences $\Delta\epsilon$ ($\text{dm}^3 \text{mol}^{-1} \text{cm}^{-1}$)

3.7 Calculated ECD and absorption spectra of each conformer (280-650 nm region)

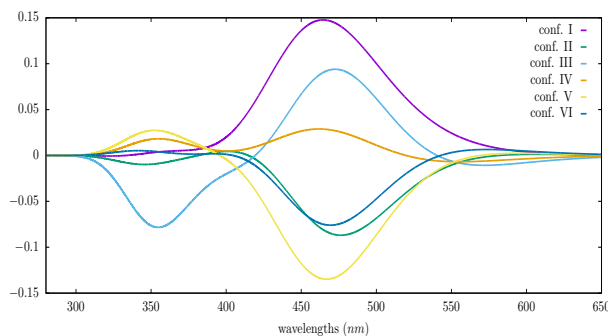


Figure SI 45: calculated ECD spectra of the six most populated conformers; calculation performed employing TD-DFT, level of theory: B3PW91/Def2TZVP; implicit solvation included through IEF-PCM (solvent:CCl₄); intensity reported as difference of molar absorption coefficients $\Delta\epsilon$ ($\text{dm}^3 \text{mol}^{-1} \text{cm}^{-1}$); FWHM: 4000 cm^{-1} (about 0.5 eV)

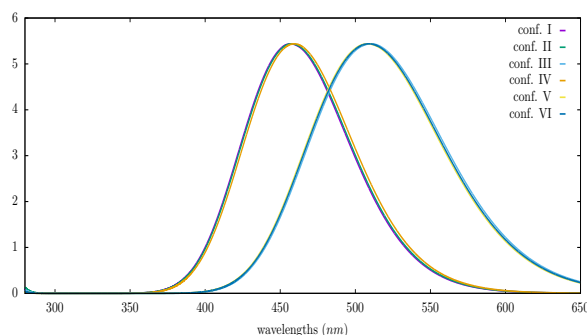


Figure SI 46: calculated absorption spectra of the six most populated conformers; calculation performed employing TD-DFT, level of theory: B3PW91/Def2TZVP; implicit solvation included through IEF-PCM (solvent:CCl₄); intensity reported as molar absorption coefficient ϵ ($\text{dm}^3 \text{mol}^{-1} \text{cm}^{-1}$); FWHM: 4000 cm^{-1} (about 0.5 eV)

3.8 Experimental ^1H NMR spectrum and assignment

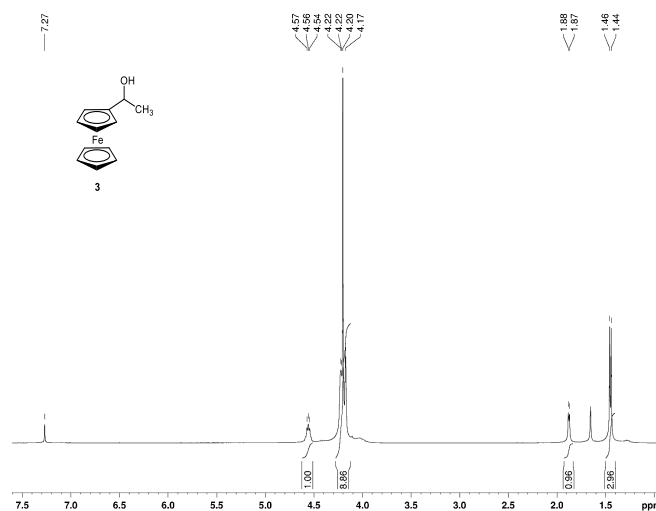


Figure SI 47: Experimental ^1H NMR spectrum of S-1-hydroxyethylferrocene

^1H -NMR (400 MHz, CDCl_3 , 0.089M): δ 1.45 (3H, d, $J = 6.4$ Hz, CH_3), 1.88 (1H, d, $J = 4.4$ Hz, OH), 4.17-4.22 (9H, m, Cp—H and Cp'—H), 4.56 (1H, m, C*—H)

3.9 coefficient of optical rotation: experimental value

$[\alpha]_D = +28.0$ (c 0.35, CHCl_3) for *S*-enantiomer, *ee* 95% (by chiral HPLC)

Reference (P. Vicennati, P.G. Cozzi, *Eur. J. Org. Chem.*, 2007, 2248-2253):

$[\alpha]_D = +31.3$ (c 0.16, CHCl_3) for *S*-enantiomer, *ee* 86%

3.10 Bond analysis on conformers I, II and III

3.10.1 Brief outline of the method

Given an adduct AB formed by fragments A and B, the electron charge rearrangement taking place after formation of the A–B bond can be formulated as the difference $\Delta\rho(x,y,z)$ between the total electron density of the adduct and a reference electron density, which is associated with the unbound fragments A and B (taken at their in-adduct geometries) and constructed from the occupied molecular orbitals of the isolated fragments previously made orthonormal to each other. If all densities are worked out from single-determinant wavefunctions (as in the present DFT calculations), by diagonalizing the so-called ‘valence operator’ and finding its eigenvalues w_k and eigenfunctions φ_k termed as ‘natural orbitals for chemical valence’ (NOCVs), $\Delta\rho$ can be decomposed into weighed contributions ascribable to pairs of NOCVs coupled by eigenvalue w_k :

$$\Delta\rho = \sum_k w_k (|\varphi_k|^2 - |\varphi_{-k}|^2) = \sum_k w_k \Delta\rho_k, \quad (1)$$

where the spatial dependence of densities and orbitals has been dropped for clarity. In other words, the total electron charge rearrangement taking place after bond formation is decomposed into additive charge flows of w_k electrons flowing from orbital φ_{-k} to orbital φ_k , with k ranging from one to the number of occupied molecular orbitals of the adduct. Only a few NOCV components in Eq. 1 have a significant weight and thus contribute non-negligibly to the overall charge rearrangement. The chemical nature (i.e., donation, backdonation, σ or π character etc.) of these contributions can be recognized by a visual inspection in 3D space of the related electron-density difference. The interested reader is referred to Refs. 1–7 for further details.

3.10.2 Computational details

To the purpose of analyzing intramolecular interactions involving the OH group in (1-hydroxyethyl)ferrocene, $\text{Fe}(\text{Cp})(\text{C}_5\text{H}_4\text{R})$ with $\text{R} = \text{CH}(\text{Me})\text{OH}$, the A and B fragments were chosen to be $[\text{Fe}(\text{Cp})]^+$ and $[(\text{C}_5\text{H}_4\text{R})]^-$ (note that the metal-ligand bonding in ferrocenes is usually discussed in terms of the interactions between Fe^{2+} and $(\text{Cp}^-)_2$ because of the aromaticity of the Cp ligand involving a six-electron occupation of its π orbitals).⁸

Bond analysis was performed on electron densities calculated in vacuum at the B3PW91/Def2TZVP level of theory by interfacing G16 with an *ad hoc* written program.⁹

3.10.3 Results

An account of the results of the bond analysis on (1-hydroxyethyl)ferrocene, conformer I, is given through Table SI 8 and Fig. SI 48: the weights of the first twelve

($k \leq 12$) contributions to the overall charge rearrangement following bond formation between $[\text{Fe}(\text{Cp})]^+$ and $[(\text{C}_5\text{H}_4\text{R})]^-$ are reported in the table, while graphical representations through isodensity-surface plots of the related NOCV orbitals are given in the figure.

Visual inspection of these plots reveals that the most important contributions ($k \leq 6$, $w_k \geq 0.19$) to the overall charge rearrangement taking place upon bonding of $[\text{Fe}(\text{Cp})]^+$ to $[(\text{C}_5\text{H}_4\text{R})]^-$ involve the interaction of the atomic orbitals of Fe with the molecular orbitals of the substituted cyclopentadienyl ring (recall that, by definition, bond formation involves a charge flow of w_k electrons from orbital φ_{-k} to orbital φ_k). The following contribution ($k = 7$, $w_k = 0.12$) involves the π electrons of the unsubstituted cyclopentadienyl ring, partly releasing charge towards the substituted-ring moiety (as also happens for $k = 8$ and 10), and partly engaging in an interaction with the H atom. The remaining contributions represent intra-fragment charge redistribution in the substituted ring ($k = 9, 11, 12$).

Results for conformers II and III, reported in Table SI 8 and Figs. SI 49-SI 50, confirm the same picture (variations in the weights w_k with respect to conformer I are ≤ 0.01) with the notable exception of the contribution with $k = 7$ for conformer III which now, due to a markedly different orientation of the OH group, does not involve an interaction between the H atom of this group and the π electrons of the unsubstituted cyclopentadienyl ring.

References

- [1] G. Bistoni, S. Rampino, F. Tarantelli, and L. Belpassi, "Charge-displacement analysis via natural orbitals for chemical valence: Charge transfer effects in coordination chemistry," *The Journal of Chemical Physics*, vol. 142, no. 8, p. 084112 (9), 2015.
- [2] M. Mitoraj and A. Michalak, "Natural orbitals for chemical valence as descriptors of chemical bonding in transition metal complexes," *Journal of Molecular Modeling*, vol. 13, no. 2, pp. 347–355, 2007.
- [3] M. Radoń, "On the properties of natural orbitals for chemical valence," *Theoretical Chemistry Accounts*, vol. 120, no. 4-6, pp. 337–339, 2008.
- [4] M. Fusè, I. Rimoldi, E. Cesarotti, S. Rampino, and V. Barone, "On the relation between carbonyl stretching frequencies and the donor power of chelating diphosphines in nickel dicarbonyl complexes," *Physical Chemistry Chemical Physics*, vol. 19, pp. 9028–9038, 2017.
- [5] M. De Santis, S. Rampino, H. M. Quiney, L. Belpassi, and L. Storchi, "Charge-displacement analysis via natural orbitals for chemical valence in the four-component relativistic framework," *Journal of Chemical Theory and Computation*, vol. 14, no. 3, pp. 1286–1296, 2018.

- [6] M. Fusè, I. Rimoldi, G. Facchetti, S. Rampino, and V. Barone, “Exploiting coordination geometry to selectively predict the σ -donor and π -acceptor abilities of ligands: a back-and-forth journey between electronic properties and spectroscopy,” *Chemical Communications*, vol. 54, pp. 2397–2400, 2018.
- [7] A. Salvadori, M. Fusè, G. Mancini, S. Rampino, and V. Barone, “Diving into chemical bonding: an immersive analysis of the electron charge rearrangement through virtual reality,” *Journal of Computational Chemistry*, 2018. <https://doi.org/10.1002/jcc.25523>.
- [8] G. Frenking, K. Wichmann, N. Fröhlich, C. Loschen, M. Lein, J. Frunzke, and M. R. Víctor, “Towards a rigorously defined quantum chemical analysis of the chemical bond in donor-acceptor complexes,” *Coordination Chemistry Reviews*, vol. 238-239, pp. 55 – 82, 2003. Theoretical and Computational Chemistry.
- [9] S. Rampino, “The Waverley program package.” <http://www.srampino.com/code.html#Waverley>. Accessed November 23, 2017.

Table SI 8: Weights (NOCV eigenvalues w_k) of the first twelve charge-rearrangement components for conformers I-III

k	w_k		
	I	II	III
1	0.76	0.76	0.76
2	0.75	0.75	0.74
3	0.39	0.39	0.40
4	0.39	0.39	0.39
5	0.23	0.23	0.23
6	0.19	0.19	0.18
7	0.12	0.12	0.11
8	0.11	0.11	0.11
9	0.10	0.10	0.10
10	0.09	0.09	0.09
11	0.08	0.08	0.08
12	0.08	0.08	0.08

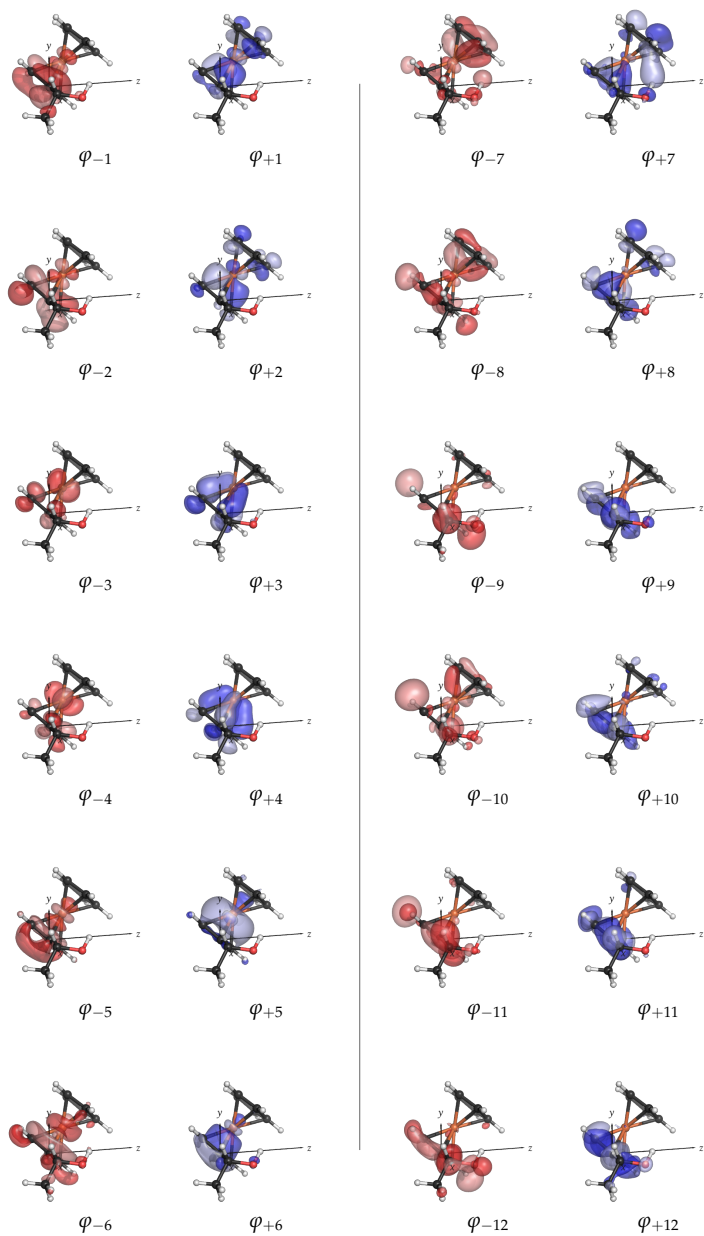


Figure SI 48: First twelve NOCV pairs (φ_{-k} and φ_k , isodensity surfaces at ± 0.05 $(e/\text{bohr}^3)^{1/2}$) for conformer I.

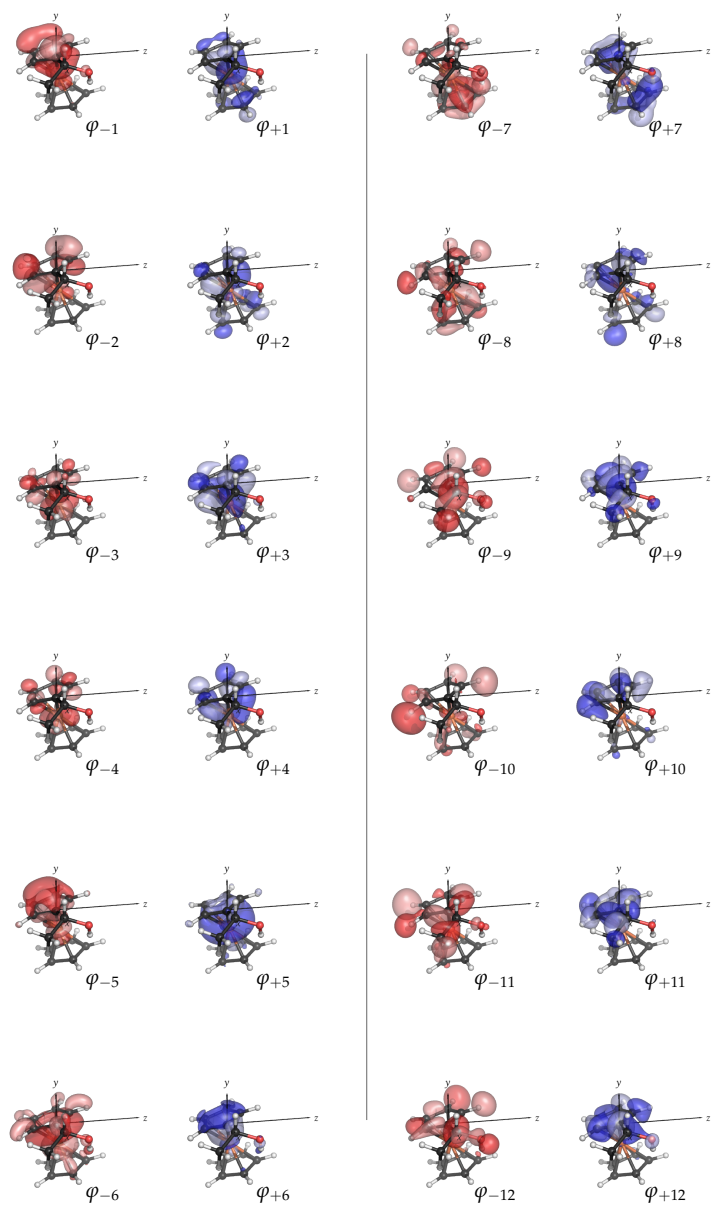


Figure SI 49: First twelve NOCV pairs (φ_{-k} and φ_k , isodensity surfaces at ± 0.05 (e/bohr^3)^{1/2}) for conformer II.

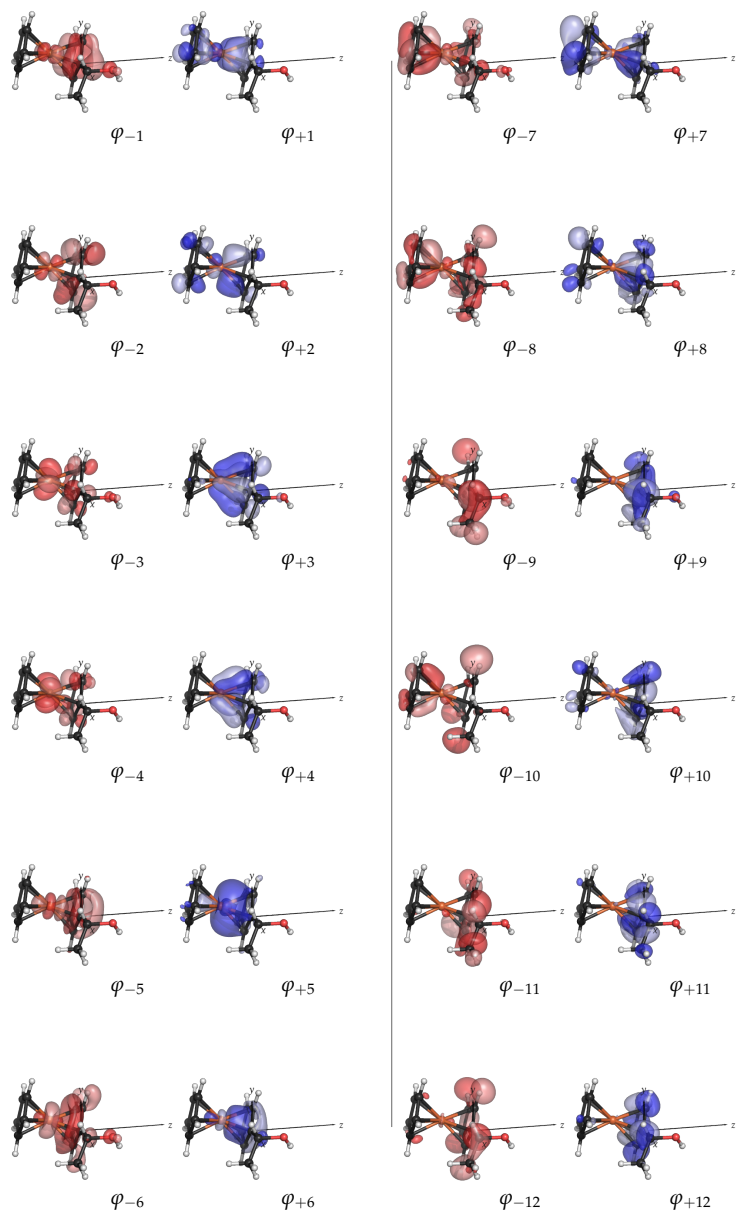


Figure SI 50: First twelve NOCV pairs (φ_{-k} and φ_k , isodensity surfaces at ± 0.05 $(e/\text{bohr}^3)^{1/2}$) for conformer III.

4 (S,S)-1,1'-bis(1-hydroxyethyl)ferrocene

4.1 Monomers

4.1.1 Structure of each conformer

In this section the structure of each conformer from different perspectives is reported; each geometry is optimized at the B3PW91/Def2TZVP level of theory.

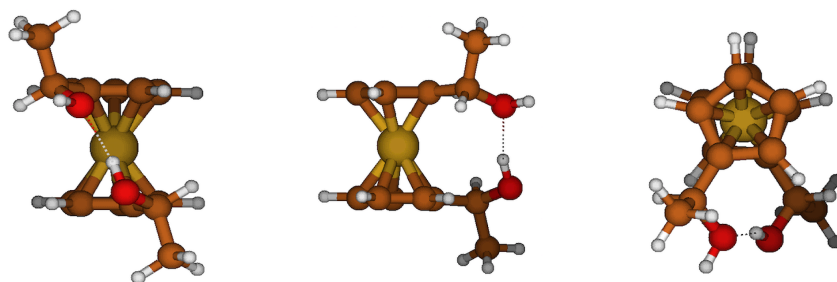


Figure SI 51: conformer I

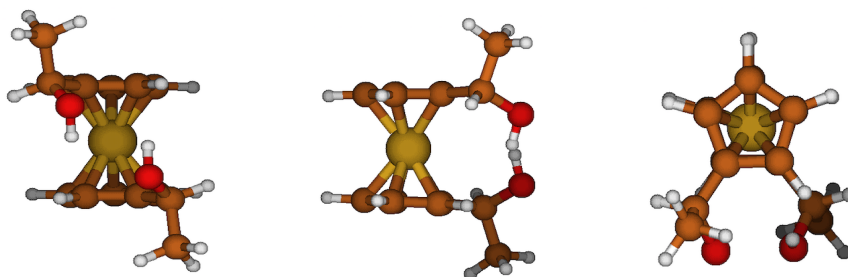


Figure SI 52: conformer II

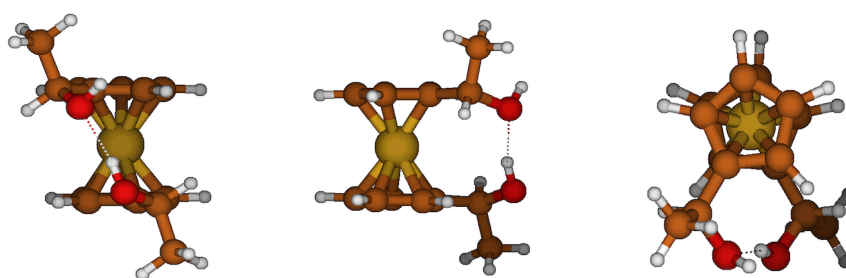


Figure SI 53: conformer III

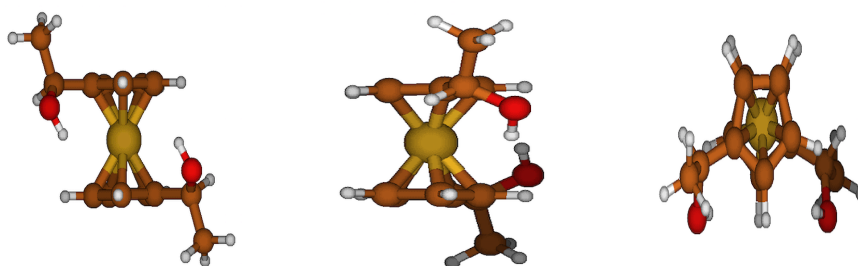


Figure SI 54: conformer IV

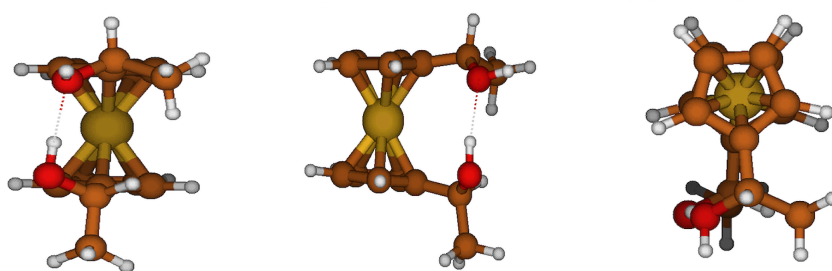


Figure SI 55: conformer V

4.2 Dimer

4.2.1 Structure

In this section the structure of the dimer from different perspectives is reported; the geometry is optimized at the B3PW91/Def2TZVP level of theory.

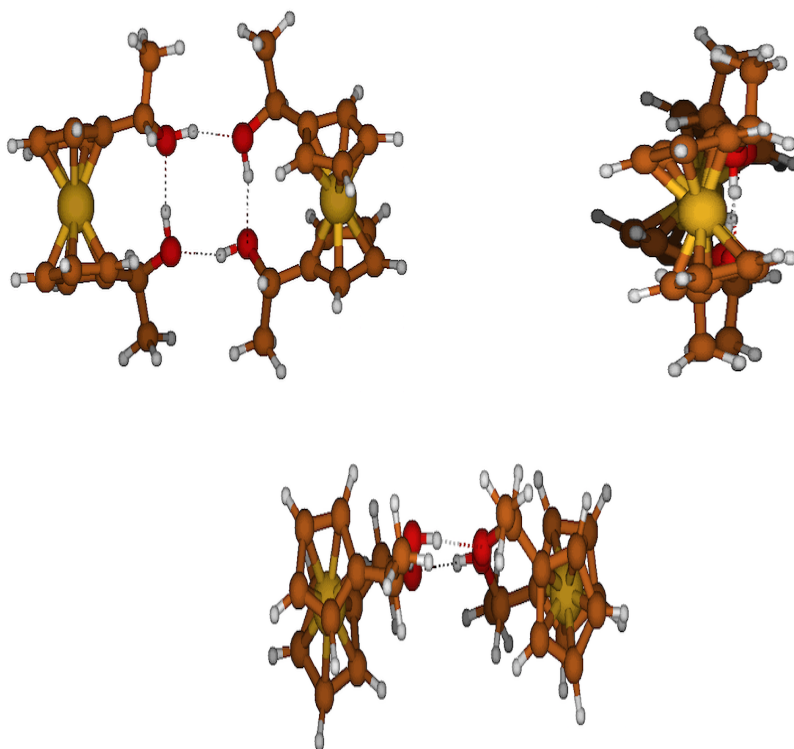


Figure SI 56: structure of the dimer

4.3 Experimental ^1H NMR spectrum and assignment

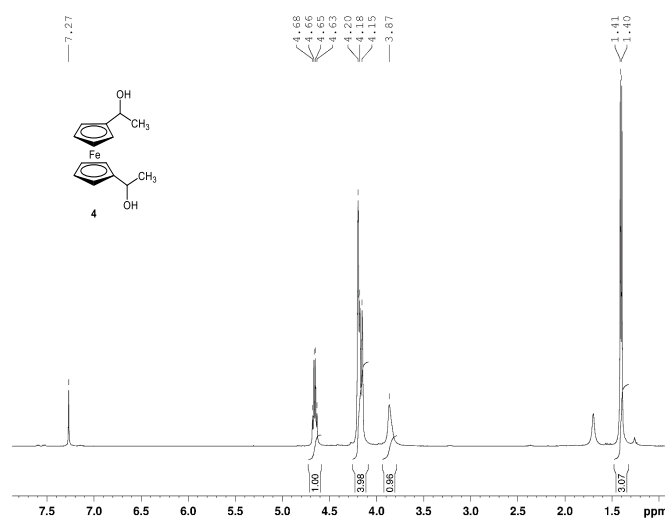


Figure SI 57: Experimental ^1H NMR spectrum of (S,S)-1,1'-bis(1-hydroxyethyl)ferrocene

^1H -NMR (400 MHz, CDCl_3 , 0.046M): δ 1.40 (6H, d, $J = 6.4$ Hz, CH_3), 3.87 (2H, br s, OH), 4.15-4.20 (8H, m, Cp—H and Cp'—H), 4.66 (2H, q, $J = 6.4$ Hz, C*—H).

4.4 coefficient of optical rotation: experimental value

$[\alpha]_D = +40.4$ (c 0.5, CHCl_3) for (S,S)-enantiomer, $ee > 98\%$, $dr > 98:2$ (by chiral HPLC)

Reference (D. Lambusta, G. Nicolosi, A. Patti, M. Piattelli, *Tetrahedron: Asymmetry*, 1993, **4**, 919-924):

$[\alpha]_D = +42.0$ (c 0.5, C_6H_6) for (S,S)-enantiomer, $ee > 99\%$, $dr > 99:1$

4.5 DOSY spectrum

The experimental DOSY spectrum of (*S,S*)-1,1'-bis(1-hydroxyethyl)ferrocene is reported in figure SI 58. From the experimental DOSY spectrum the value of $1.08 \cdot 10^{-9} \text{m}^2 \cdot \text{s}^{-1}$ for the diffusion coefficient has been obtained for a solution of concentration 0.03 M of the diol in chloroform. Applying the Stokes-Einstein equation (see eq. 2), valid for the diffusion of a spherical particle through a liquid with low Reynolds number, a radius (r_H) of 3.83 Å has been calculated (the other values used in the equation are: $T = 298\text{K}$; $\eta = 5.28 \cdot 10^{-4} \text{Pa} \cdot \text{s}$ and $k = 1.38065 \cdot 10^{-23} \text{J} \cdot \text{K}^{-1}$).

$$D = \frac{KT}{6\pi\eta r_H} \quad (2)$$

A rough estimate of the molecular volume of monomer and dimer of the diol can be obtained from the computational data reported and discussed in the main article and in the previous sections of SI. The molecular volume estimated by constructing an ellipsoid on the basis of the optimized geometry of the most populated conformer of the monomer is equal to 49.9Å^3 , while the molecular volume estimated in the same way for the dimer is of 225.9Å^3 . If these molecular volumes are associated to spheres, values of the radius may be obtained through $r_M = \left(\frac{3V}{4\pi}\right)^{\frac{1}{3}}$ and are equal to 2.28 Å for the monomer and 3.78 Å for the dimer. These rough estimates obtained on the basis of the calculated geometries of the two systems supports the assignment of the experimental signal of the DOSY spectrum to the dimer.

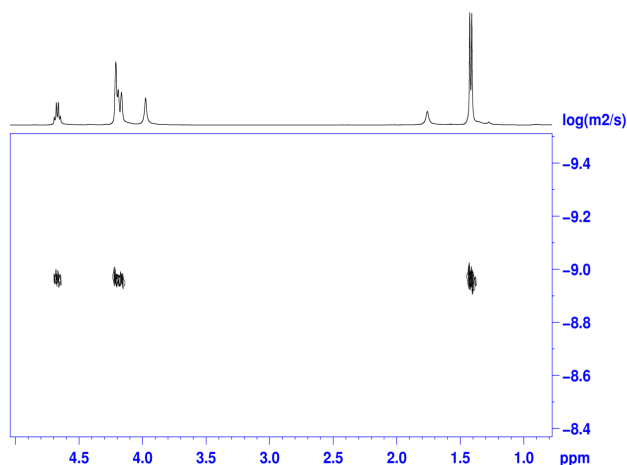


Figure SI 58: Experimental DOSY spectrum of (*S,S*)-1,1'-bis(1-hydroxyethyl)ferrocene